Active-Site-Directed Photolabeling of the Melibiose Permease of *Escherichia coli*†

Yves Ambroise,‡ Gérard Leblanc,§ and Bernard Rousseau*,‡

Service des Molécules Marquées, Département de Biologie Cellulaire et Moléculaire, CEA/Saclay, 91191 Gif sur Yvette Cedex, France, and Laboratoire de Physiologie des Membranes Cellulaires, LRC-CEA 16V, Université de Nice Sophia-Antipolis and CNRS (ERS 1253), 06238 Villefranche sur Mer Cedex, France

Received July 14, 1999; Revised Manuscript Received October 18, 1999

ABSTRACT: Covalent photolabeling of the melibiose permease (MelB) of *Escherichia coli* has been undertaken with the sugar analogue [^{3}H]-*p*-azidophenyl α-D-galactopyranoside ([^{3}H]-α-PAPG) with the purpose of identifying the domains forming the MelB sugar-binding site. We show that α-PAPG is a high-affinity substrate of MelB ($K_d = 1 \times 10^{-6}$ M). Its binding to or transport by MelB is Na-dependent and is competitively prevented by melibiose or by the high-affinity ligand *p*-nitrophenyl α-D-galactopyranoside (α-NPG). Membrane vesicles containing overexpressed histidine-tagged recombinant MelB were photolabeled in the presence of [^{3}H]-α-PAPG by irradiation with UV light ($\lambda = 250$ nm). Eighty-five percent of the radioactivity covalently associated with the vesicles was incorporated in a polypeptide corresponding to MelB monomer. MelB labeling was completely prevented by an excess of melibiose or α-NPG during the assay. Radioactivity analysis of CNBr cleavage or limited proteolysis products of the purified [^{3}H]-α-PAPG-labeled transporter suggests that several domains of MelB are targets for labeling. One of the labeled CNBr cleavage products is a peptide with an apparent molecular mass of 5.5 kDa. It is shown that (i) its amino acid sequence is that of the Asp124−Met181 domain of MelB (7.5 kDa), which includes the cytoplasmic loop 4−5 connecting helices IV and V, the hydrophobic helix V, and the outer loop connecting helices V−VI, and (ii) that Arg141 in loop 4−5 is the only labeled amino acid of this peptide. Labeling of loop 4−5 provides independent evidence that this specific domain plays a significant role in MelB transport. Comparison with the well-characterized equivalent domain of LacY suggests that sugar transporters with similar structure and substrate specificity may have conserved domains involved in sugar recognition.

The melibiose permease (MelB)[1] of *Escherichia coli*, encoded by *melB*, catalyzes the accumulation of a variety of α-galactosides (melibiose, α-NPG) in association with either Na^+, H^+, or Li^+ by a cation/sugar symport mechanism [reviewed by Pourcher et al. (*1*) and Poolman et al. (*2*)]. MelB is a highly hydrophobic membrane transporter of 473 amino acids (*3*, *4*) that is among the best-studied co-transporters of the Na^+/solute symporter family (*5*, *6*). A topological model of MelB consisting of 12 transmembrane α-helices has received independent support from a variety of experimental approaches, including *pho*A fusion analysis (*7*, *8*) and proteolytic digestion experiments (*9*). The purification of large amounts of homogeneous MelB (*4*) has enhanced the prospects for structural studies using, for example, spectroscopy (*10*, *11*) and crystallography (*12*).

Although the basic features of the ion-coupled sugar transport by MelB are satisfactorily described kinetically (*13*, *1*), the molecular mechanisms underlying the ionic or sugar specificity, or that by which the flows of the two substrates are coupled during transport, are still poorly understood. Answers to these fundamental questions require, in addition to other information, a better topological and/or structural description of the functional organization of the transporter. Identification of the domains forming the sugar- and cation-binding sites of MelB and their relationship is still fragmentary. Thus, site-directed mutagenesis of the *melB* gene (*14*−*16*) and construction of chimeric melibiose transporters from various microorganisms (*17*) have led to the concept that the N-terminal transmembrane domains of MelB may accommodate the ion-binding site, or at least part of it. On the other hand, in vitro mutagenesis, combined with fluorescence spectroscopy analysis, suggests the proximity of Trp342 (located in the C-terminal half of MelB) to the sugar-binding site (*18*, *19*). However, these proposals are not unequivocal, as detailed characterization of these and many other MelB mutants indicate that point mutations of MelB often result in more than one change in the functional properties of the transporter, such as the concomitant modification of its ionic and sugar selectivity properties (*20*).

† This work was supported in part by Grant BioC4-CT97-2119 from the European Commission to G.L.

* To whom correspondence should be addressed: Tel 33-1-69-08-54-93; Fax 33-1-69-08-79-91; e-mail bernard.rousseau@cea.fr.

‡ CEA/Saclay.

§ Université de Nice Sophia-Antipolis.

[1] Abbreviations: MelB, melibiose permease; -PAPG, *p*-azidophenyl D-galactopyranoside; -NPG, *p*-nitrophenyl D-galactopyranoside; Ni−NTA, nickel−nitrilotriacetic acid; MW, molecular weight; LAPAO, lauryl(aminopropyl)diamine *N*-oxide; NMR, nuclear magnetic resonance; HPLC, high-performance liquid chromatography; MS, mass spectrometry; TFA, trifluoroacetic acid; RSO, right side out; IMVs, inverted membrane vesicles; ClCCP, carbonyl cyanide *p*-(trichloromethoxy)phenylhydrazone; K_d, dissociation constant; B_{max}, maximal number of binding sites; SDS, sodium dodecyl sulfate; PAGE, polyacrylamide gel electrophoresis; PVDF, poly(vinylidene difluoride); CAPS, 3-(cyclohexylamino)-1-propanesulfonic acid; Pk, proteinase K; Ti, trypsin; PTH, phenylthiohydantoin.

10.1021/bi9916224 CCC: $19.00
Published on Web 01/19/2000

Active-site-directed labeling of proteins, and particularly photodependent labeling, is a strategy of choice to identify the domains and/or residues directly participating in the substrate−protein interaction (*21*). This approach requires chemical engineering of photoreactive substrates displaying good affinity. In this respect, MelB has a broad sugar selectivity and displays micromolar affinity toward galactopyranosyl analogues carrying an aromatic moiety on the C1-OH, such as nitrophenyl-α-galactosides (*22*) or dansyl galactosides (*11*). The high-affinity ligand [^{3}H]-*p*-nitrophenyl α-D-galactopyranoside has already been used to photolabel and identify the lactose permease (LacY) of *Escherichia coli* (*23*, *24*). However, LacY photolabeling could not be exploited to gain insight into the functional organization of the permease, as nitrobenzenes with no leaving group (-OR, -X) on the ring are not very reliable as photolabeling reagents (*25*), and also as the photolabel incorporation was unstable upon LacY solubilization in detergents (*24*).

In the present study, we used the nitrene-based photoactivatable sugar analogue *p*-azidophenyl α-D-galactopyranoside (α-PAPG) to map the sugar-binding site of MelB. It is first shown that this sugar analogue is a high-affinity substrate of MelB. Photolabeling of the transporter with [^{3}H]-α-PAPG was carried out in membrane vesicles harboring high levels of a recombinant MelB-6His transporter (*4*) that enable subsequent purification and biochemical analysis of the labeled transporter polypeptide. The sites of covalent labeling by [^{3}H]-α-PAPG were analyzed after cyanogen bromide cleavage by peptide sequencing. The data indicate that the cytoplasmic loop connecting helices IV−V, and more precisely Arg141, is one of the labeling targets of [^{3}H]-α-PAPG. Finally, limited proteolytic analysis of the [^{3}H]-α-PAPG-labeled MelB suggests additional labeling sites.

MATERIALS AND METHODS

Materials. All reagents were electrophoretic or sequencing grade and were from Sigma or Aldrich. Electrophoresis materials and protein standards were from Bio-Rad. Autoradiography film, Amplify, Lipoluma, and Lumasolve scintillation cocktails were from Amersham. Ni−NTA on agarose was from Qiagen. [^{3}H]-α-NPG (14 Ci/mmol, 1 mCi/mL in EtOH) was prepared from α-NPG by selective oxidation of the galactose moiety at position C-6 by a galactose oxidase assay and subsequent reduction with KB-[^{3}H]$_4$. The detergent lauryl(aminopropyl)diamine *N*-oxide (LAPAO) was synthesized as described by Brandolin et al. (*26*).

Synthesis of [^{3}H]-α-PAPG. [^{3}H]-α-PAPG (25 Ci/mmol, 1 mCi/mL in H_2O/EtOH = 90/10) was prepared from *p*-aminophenyl α-D-galactopyranoside by a three-step procedure. The phenyl ring of *p*-aminophenyl α-D-galactopyranoside was first brominated with Br_2 in AcOH. [^{3}H]-*p*-Aminophenyl α-D-galactopyranoside was then obtained by catalytic dehalogenation in the presence of Pd/C and tritium gas. Finally, [^{3}H]-α-PAPG was obtained by diazotation of the primary amine with $NaNO_2$/AcOH followed by NaN_3 treatment and subsequent purification on a Zorbax-ODS HPLC column. ^{3}H NMR showed a single tritium labeling position at the phenyl moiety. [^{3}H]-α-PAPG synthesis will be described in detail elsewhere. [^{3}H]-α-PAPG (25 Ci/mmol estimated by MS) was stored in H_2O/EtOH (90/10) at 1 mCi/mL. Before use, the purity of the labeled analogue was checked by reversed-phase HPLC on a Zorbax-ODS column (4.6 × 25 mm) with MeOH/H_2O/TFA (20/80/0.1%) as the mobile phase at a flow rate of 1 mL/min. Elution was monitored by UV absorbance at 250 nm and direct flowthrough radioactive detection (LB 504 from EG&G). [^{3}H]-α-PAPG was detected as a single peak at 15.8 min and coeluted with nonradioactive α-PAPG.

Preparation of Membrane Vesicles. DW2/pK*melB*-6His cells grown to mid-log phase were used to prepare right-side-out (RSO) vesicles or inverted membrane vesicles (IMVs). RSO membrane vesicles were prepared according to Kaback (*27*) and resuspended in Na-free 0.1 M potassium phosphate medium, pH 7.0. IMVs were prepared by means of a French press cell at 20 000 psi (American Instrument Company) as described by Pourcher et al. (*4*), resuspended in 50 mM Tris and 50 mM NaCl buffer (pH 8.0) at a final concentration of 30 mg/mL, and frozen until used.

Transport and Binding Assays. Because lipophilic analogues of galactose such as α-PAPG diffuse rapidly across membranes, active [^{3}H]-α-PAPG (1 μM, 25 Ci/mmol) transport in RSO membrane vesicles (1.8 mg of protein/mL) was best measured by means of the flow dialysis procedure described by Ramos et al. (*28*). RSO membrane vesicles were energized by adding phenazine methosulfate (0.2 mM) reduced by ascorbic acid (20 mM), and collapse of the resulting protonmotive force was achieved by adding valinomycin at a final concentration of 5 μM. Binding of [^{3}H]-α-PAPG to inverted membrane vesicles was assayed under nonenergized conditions by flow dialysis (*22*). Initially, the upper chamber of the flow dialysis cell contained 0.3 mL of vesicle suspension (2−6 mg of protein/mL), as well as monensin (0.75 μM) and carbonyl cyanide *p*-(trichloromethoxy)phenylhydrazone (ClCCP, 5 μM) to ensure complete membrane de-energization and [^{3}H]-α-PAPG (1 μM, 25 Ci/mmol). [^{3}H]-α-PAPG binding was studied as a function of free α-PAPG (1−5 μM) through stepwise addition of unlabeled ligand to the vesicle suspension. Binding constants, i.e., dissociation constant K_d and maximal number of binding sites (B_{max}), were calculated as described by Damiano-Forano et al. (*22*).

Photolabeling of MelB in Vesicles with [^{3}H]-α-PAPG. Photolabeling of MelB in IMVs with [^{3}H]-α-PAPG was carried out on an analytical or preparative scale. Membrane vesicles, corresponding to 1 or 4 nmol of total active MelB, were suspended in 50 mM Tris-HCl (pH 8.0) containing 50 mM NaCl, [^{3}H]-α-PAPG (5 μM), monensin (0.75 μM), and ClCCP (5 μM). The alcohol concentration never exceeded 1% (v/v) of the total buffer volume. The membrane suspension was incubated for 60 min in the dark at 4 °C, then placed in a 3 mL UV cell thermostated at 18 °C and irradiated with a 1000 W Müller Lax 1000 Xe/Hg lamp connected to a monochromator. The light beam at $\lambda = 250$ nm was focused with a lens to a spot about 10 mm high and 2 mm wide, and the resulting energy was measured with an International Light IL 1700 radiometer. The apparatus was equilibrated to provide a constant energy of $E = 5 \times 10^{-5}$ mW·cm^{-2} throughout the experiments.

Quantitative Measurements of Radioactivity Incorporation in MelB. Immediately after photolysis, two aliquots of the membrane vesicles were solubilized in 1% SDS and proteins were separated by SDS−PAGE on 12% acrylamide minigels

(*29*). One of the gels was stained with Coomassie Blue and destained in 10% acetic acid and 40% methanol in water. The gel was sliced into 2 mm pieces and each piece was subsequently digested in 10 mL of Lipoluma/Lumasolve (90/10) overnight at 60 °C and counted in a Wallac 1409 liquid scintillation counter (EG&G) with internal standard. The second gel was fixed for 30 min in 10% acetic acid and 40% methanol in water, shaken for 15 min with Amplify (Amersham), dried under vacuum, and finally autoradiographed with Hyperfilm-MP (Amersham) for 24 h at −80 °C.

Purification of Labeled MelB. The procedure used for purification of labeled His-tagged MelB was essentially that described by Pourcher et al. (*4*). Basically, photolabeled vesicles were solubilized in the presence of lauryl (aminopropyl)diamine *N*-oxide (LAPAO) and NaCl at respective final concentrations of 1% and 250 mM. The supernatant was equilibrated for 1 h at 4 °C with Ni−NTA resin and washed four times with 50 mM Tris-HCl (pH 8), 250 mM NaCl, 0.1% LAPAO, and 10 mM imidazole to remove most contaminants. The remaining adsorbed protein containing up to 95% of MelB was eluted by raising the imidazole concentration to 250 mM.

CNBr Cleavage and Electroblotting of Photolabeled MelB Fragments. Photolabeled MelB purified by Ni−NTA chromatography was precipitated with cold 10% trichloroacetic acid at 4 °C for 30 min. The pellet was then washed twice with cold acetone. The precipitated material was subjected to CNBr fragmentation in 70% formic acid for 16 h at 37 °C and finally evaporated to dryness with a Speedvac apparatus. The CNBr dried digest solubilized in 1% SDS was run on a 5−16.5% Tris−Tricine gel system (*30*) and electroblotted immediately onto a PVDF membrane (Sequi-Blot from Bio-Rad) in 10 mM CAPS transfer buffer containing 10% methanol. The PVDF membrane was washed with water, stained in 0.1% Ponceau S (1% acetic acid in water) for 1 min, and destained in NaOH (10^{-3} M). The pieces of PVDF membrane carrying radioactive bands were excised and used for N-terminal sequencing (Applied Biosystems 477 A protein sequencer equipped with an on-line HPLC 120 A). For each sequencing cycle, 30% of the fraction collected was analyzed in the on-line PTH analyzer for PTH derivative release, while the remaining 70% was counted for [^{3}H] release. All experiments were carried out in duplicate.

Protein Determination. Protein concentration was determined according to Lowry et al. (*31*).

RESULTS

Photolysis Properties of α*-PAPG*. α-PAPG prepared at 100 μM in 50 mM Tris-HCl and 50 mM NaCl (pH 8.0) solution has a UV absorption spectrum dominated by a maximum at $\lambda = 250$ nm (Figure 1). α-PAPG photolysis characteristics were analyzed by recording its UV absorption spectrum after different times of illumination with a monochromatic light at $\lambda = 250$ nm with a power beam of $E = 5 \times 10^{-5}$ mW·cm^{-2} (Figure 1). The time course of variation of the absorption peak at $\lambda = 250$ nm was plotted and the photolysis half-time was calculated graphically (inset, Figure 1). Under the above conditions of illumination, the $t_{1/2}$ was 70 s. In contrast, α-NPG was not altered even after 60 min of illumination at $E = 5 \times 10^{-4}$ mW·cm^{-2}. Brief illumination did not significantly change the sugar-binding capacity of the membrane vesicles in the absence of probe during the assay.

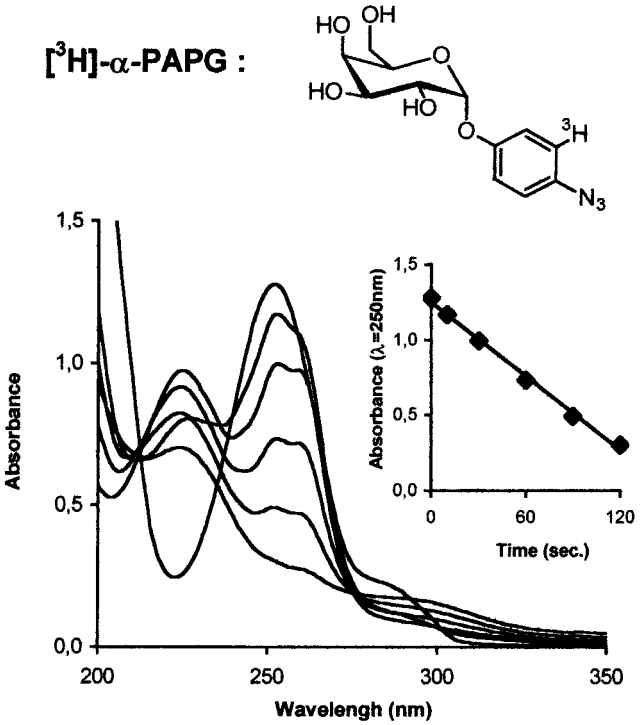

FIGURE 1: Time course of photolysis of [^{3}H]-α-PAPG. Aliquots (500 μL) of a buffered solution (50 mM Tris and 50 mM NaCl, pH 8) of [^{3}H]-α-PAPG (100 μM) were irradiated at $\lambda = 250$ nm, $E = 5 \times 10^{-5}$ mW·cm^{-2}, and 18 °C. Absorbance spectra were recorded between 200 and 350 nm immediately after 0, 10, 30, 60, 90 or 120 s of illumination. Inset: Time course of photolysis of [^{3}H]-α-PAPG at $\lambda = 250$ nm. The structure of [^{3}H]-α-PAPG is shown at the top.

*[^{3}H]-*α*-PAPG Is a High-Affinity Substrate of MelB.* α-PAPG must be a good substrate of the transporter if it is to be used as a tool to map the sugar-binding site of MelB by a photolabeling approach. The characteristics of [^{3}H]-α-PAPG accumulation by RSO membrane vesicles expressing a His-tagged MelB (MelB-6His) were first investigated by a flow dialysis assay, which minimizes the inconvenience of a high rate of lipophilic substrate redistribution across the *E. coli* membrane (*28*) (Figure 2, curve a). It is observed that addition of electron donors to the RSO membrane vesicles suspension incubated in the presence of 1 μM [^{3}H]-α-PAPG and 10 mM NaCl leads to a reduction of the sugar concentration in the outer medium, indicating accumulation in the vesicles. Almost no α-PAPG accumulation was observed in the absence of external NaCl or if melibiose was present at high concentration in the medium (not shown). Moreover, the accumulated radioactivity is released on dissipating the transmembrane electrochemical H^+ gradient with valinomycin. These data strongly suggest that the probe is accumulated by MelB.

Analysis of [^{3}H]-α-PAPG binding on RSO membrane vesicles by the flow dialysis procedure further indicates that MelB has a high affinity for this sugar analogue. This property is illustrated in Figure 2 (curve b). It is observed that addition of NaCl to de-energized RSO membrane vesicles promotes binding of [^{3}H]-α-PAPG, whereas addition of excess melibiose displaces the bound ligand. α-PAPG

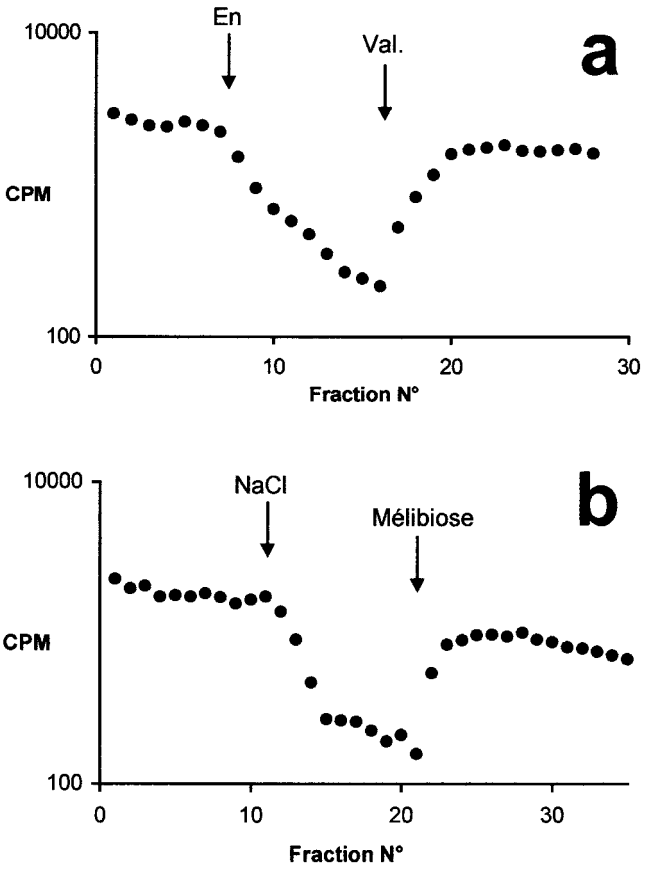

FIGURE 2: Transport or binding of [^{3}H]-α-PAPG. [^{3}H]-α-PAPG accumulation into RSO membrane vesicles was monitored by flow dialysis (curve a). RSO membrane vesicles (1.8 mg/mL) were incubated in the upper chamber of the flow dialysis apparatus containing 100 mM potassium phosphate buffer, [^{3}H]-α-PAPG (1 μM, 25 Ci/mM), and NaCl (10 mM). Ordinate: radioactivity collected in the lower chamber that measures the extravesicular concentration of sugar analogue (S_{out}). Arrow (En): Reduction of the S_{out} consecutive to sugar uptake triggered by energization of the vesicles with reduced phenazine methosulfate. Arrow (Val): increase in S_{out} that follows the release of accumulated α-PAPG when the membrane vesicles are de-energized with valinomycin (5 μM). Curve b: Binding of [^{3}H]-α-PAPG was also assayed by the flow dialysis procedure with de-energized membrane vesicles. (*22*). RSO membrane vesicles (2 mg/mL) were incubated in 100 mM potassium phosphate buffer, [^{3}H]-α-PAPG (1 μM, 25 Ci/mM), and the protonophore FCCP (5 μM) to fully de-energize the membrane vesicles. First arrow: NaCl was added at a final concentration of 10 mM. Second arrow: addition of melibiose at a final concentration of 20 mM.

binding was measured as a function of ligand concentration and in the presence of increasing concentrations of melibiose. Analysis of the data according to Eadie−Hofstee indicates that the [^{3}H]-α-PAPG binding constant (K_d) is 1 μM. [^{3}H]-α-PAPG binding is also competitively inhibited by the high-affinity ligands α-NPG and melibiose. The affinity of MelB for α-PAPG compares well with that of other galactose analogues (e.g., α-NPG, $K_d = 0.7$ μM) grafted with aromatic groups, reflecting an enhanced sugar−permease interaction (*11*). Taken together, these data indicate that α-PAPG is an Na-dependent, high-affinity substrate of MelB.

MelB Photolabeling with [^{3}H]-α-PAPG. Illumination of α-PAPG in solution by an intense monochromatic light beam at $\lambda = 250$ nm ($E = 5 \times 10^{-5}$ mW·cm^{-2}) indicated that the reactive sugar was photolyzed with a $t_{1/2}$ of about 70 s (see

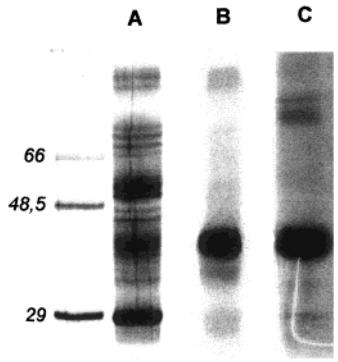

FIGURE 3: Polyacrylamide gel electrophoresis and autoradiography of photolabeled MelB in IMVs and after purification. IMVs were irradiated for 1 min with [^{3}H]-α-PAPG at $\lambda = 250$ nm, $E = 5 \times 10^{-5}$ mW·cm^{-2}, and 18 °C. Immediately after illumination, an aliquot of IMVs (25 μg) was subjected to SDS−6−12% PAGE and stained with Coomassie Blue (**A**). An identical gel was incubated in Amplify, dried, and autoradiographed for 24 h at −80 °C (**B**). MelB was purified from photolabeled IMVs as described under Materials and Methods. A 10 μg aliquot of purified MelB was analyzed on an SDS−12% SDS polyacrylamide gel and stained with Coomassie Blue (**C**).

Figure 1). Accordingly, [^{3}H]-α-PAPG incorporation in IMVs or MelB was studied during a relatively short light exposure (1−5 min). The very high rate of equilibration of the lipophilic probe across the membrane gave similar results in RSO membrane vesicles or IMVs. Although not shown, it is important to mention that the sugar-binding activity of MelB is not modified under the photolabeling conditions used. MelB photolabeling was carried out with IMV samples (1 nmol of MelB per assay) incubated in the presence of a 5-fold excess of [^{3}H]-α-PAPG (5 μM, 25 Ci/mmol), i.e. at a concentration equivalent to 5 times its K_d. The pattern of light-induced radioactivity incorporation in IMVs was examined after electrophoretic separation of the solubilized membrane proteins and subsequent autoradiography (Figure 3, lanes A and B). The sliced gel from IMVs illuminated for 1 min indicated that 85% of the ^{3}H label was associated with a polypeptide migrating at 40−43 kDa. This protein has been previously identified as the monomeric form of MelB (*4*, *9*). In comparison, none of the IMV proteins were labeled if samples were kept in the dark for 60 min. Additional characterization of the photolabeling reaction was carried out by analyzing the time course of radioactivity incorporation in the MelB polypeptide (Figure 4). The control experiment shows that the amount of label covalently attached to MelB reached a maximum after about 40 s and then remained stable. Almost complete protection against MelB labeling was observed when melibiose or α-NPG was present at a concentration about 150 times K_d (50 mM or 100 μM, respectively). In contrast, addition of sucrose, a poor MelB substrate, at a concentration of 50 mM during the photolabeling assay did not afford any significant protection against ^{3}H incorporation in the MelB band. Strong evidence that the polypeptide highly labeled by [^{3}H]-α-PAPG was MelB was obtained by purifying labeled MelB-6His by an affinity chromatography procedure involving the use of Ni−NTA resin (Figure 3, lane C). The autoradiogram (data not shown) and radioactivity profile of the gel (Figure 5) show that a very high level of radioactivity is associated with the dominating monomeric form of MelB (90%) and a residual

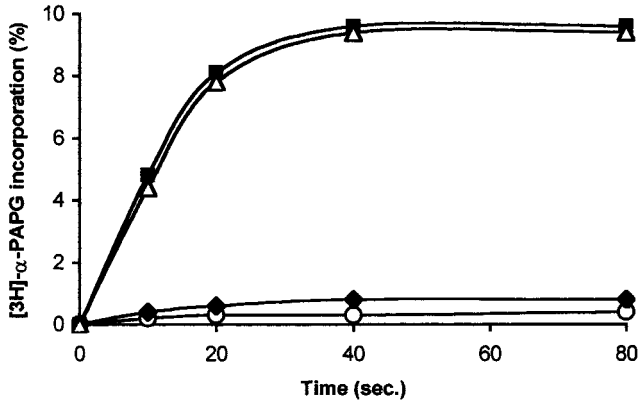

FIGURE 4: Kinetics of MelB photolabeling in membrane vesicles by [^{3}H]-α-PAPG. Irradiation was performed at $\lambda = 250$ nm and $E = 5 \times 10^{-5}$ mW·cm^{-2} with 5 μM [^{3}H]-α-PAPG (■), 5 μM [^{3}H]-α-PAPG and 50 mM melibiose (◆), 5 μM [^{3}H]-α-PAPG and 100 mM α-NPG (○), or 5 μM [^{3}H]-α-PAPG and 50 mM sucrose (△). Aliquots (100 μL) were sampled at 0, 10, 20, 40, 80, 140, 220, and 320 s, and subsequent SDS−6−12% PAGE followed by scintillation counting of MelB-containing slices gave the rate insertion of [^{3}H]-α-PAPG on MelB.

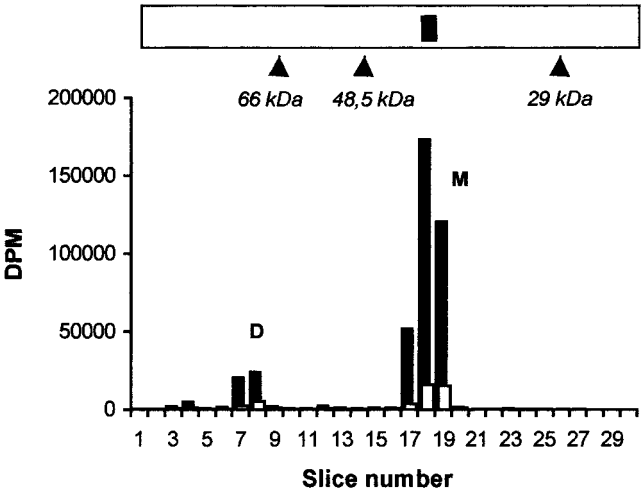

FIGURE 5: Quantitative measurement of radioactivity incorporation in MelB. IMVs (1 nmol of active sites) were incubated in the presence of [^{3}H]-α-PAPG (5 nmol, 25 Ci/mmol) and irradiated at 250 nm for 1 min as detailed under Materials and Methods. Immediately after illumination, labeled His-tagged MelB was purified on a Ni−NTA resin. An aliquot (3.2 μg) was analyzed on an SDS−6−12% polyacrylamide gel. The gel was stained with Coomassie Blue and sliced into 2 mm pieces, each of which was counted for [^{3}H] (solid bars). In a control experiment, 100 μM of α-NPG was added during illumination (open bars). The schematic representation of the Coomassie staining pattern is shown in the upper part of the figure, highlighting the position of the MelB monomer (M) and dimer (D). The arrowheads indicate the positions of standard molecular mass markers.

labeling of the dimers (10%). From the amount of purified protein and the level of labeling, it is calculated that MelB labeling efficiency is 10% (±2%). Moreover, MelB was no longer photolabeled when α-NPG was present at a final concentration of 100 μM during the assay.

Identification of the Photolabeled Domains or Sites. CNBr cleavage of the purified photolabeled MelB coupled to subsequent sequencing of the NH_2-terminus of derived peptides was chosen as a strategy to identify the domains and/or individual residues that are the targets for [^{3}H]-α-PAPG attachment. IMV samples containing up to 4 nmol of

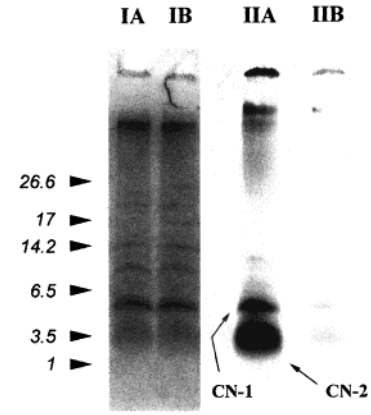

FIGURE 6: Tris−Tricine SDS−PAGE of CNBr digestion of [^{3}H]-α-PAPG-labeled MelB. MelB (4 nmol of active sites) in IMVs was photolabeled with [^{3}H]-PAPG (20 nmol, 25 Ci/mmol) as described in Figure 5, purified, and precipitated in 10% TCA. The pellet was resuspended in 100 μL of 70% formic acid and reacted with CNBr (2 mg) for 16 h at 37 °C. The reaction medium was then evaporated to dryness. The CNBr digest was analyzed on a 5−16.5% Tris−Tricine gel system as described by Schägger and von Jagow (*30*) and stained with Coomassie Blue (**IA**). The gel was equilibrated with Amplify, dried, and autoradiographed for 48 h at −80 °C (**IIA**). In a control experiment, α-NPG (100 μM) was present during the 1-min photolabeling (**IB**, Coomassie Blue-stained gel; **IIB**, [^{3}H] pattern).

MelB were photolabeled to obtain sufficient material for peptide NH_2-terminal sequencing. The peptides generated by CNBr cleavage were separated by gel electrophoresis using a 5−16.5% Tris−Tricine gel system (Figure 6) (*30*). Gel autoradiography indicated two radioactive bands (Figure 6, lane IIA). One of them was a well-resolved band of apparent molecular mass 5.5 kDa (CN-1 fragment). The other (CN-2 fragments) migrated as a broad band (2−4 kDa), suggesting that it consists of a mixture of peptides. These two bands were no longer radioactive when IMVs were photolabeled in the presence of excess α-NPG. The peptides—or peptide mixture—belonging to these two bands could be revealed with Ponceau S red after electroblotting onto a PVDF membrane. The CN-1 and CN-2 bands were cut from the PVDF membrane and subjected to Edman degradation. The CN-1 band was sequenced up to 29 cycles, beyond which the PTH derivative signal was too low to make a definitive assignment. The determined CN-1 sequence matches exactly the MelB sequence between Asp124 and Ala152, suggesting that the CN-1 peptide (with an apparent molecular mass of 5.5 kDa) corresponds to the Asp124−Met181 domain of MelB of 7.5 kDa. The anomalous rate of migration of this peptide may be related to an elevated hydrophobicity. Moreover, the totality of the radioactivity loaded onto the membrane support was released at the 18th cycle (Arg141), while PTH-Arg was detected by on-line HPLC (data not shown). As no additional radioactivity was released during the initial washing procedure, nor bound to membrane support at the end of the analysis, the data demonstrated that the radioactivity was only associated with Arg141. Sequencing the broad CN-2 band indicated the presence of at least two major peptides that could be fully sequenced. The first corresponds to the MelB stretch Val349−Met374 and the other to Ile394−Met410. However, these peptides did not carry any significant radioactivity. The radioactivity associated with the CN-2 sample remaining on the sequencing

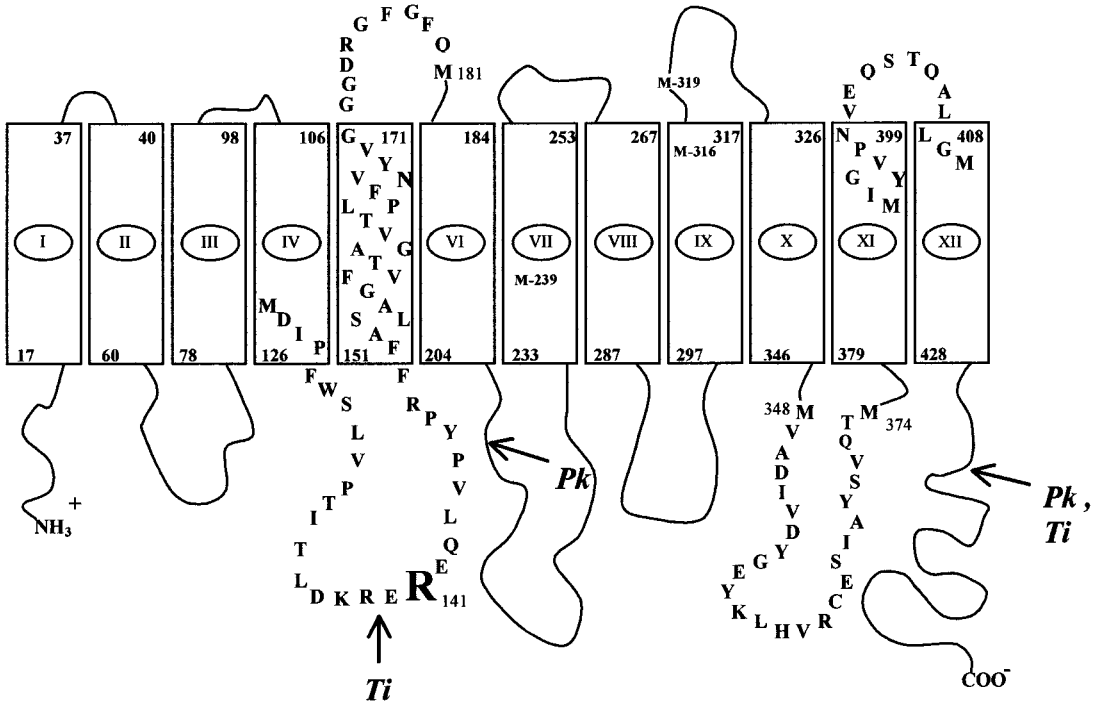

FIGURE 7: Location of the three sequenced CNBr cleavage products on the topological model of MelB. The secondary structure model of MelB illustrated is from Pourcher et al. (*7*). Transmembrane helical domain is represented by rectangles and numbered by circled roman numbers. Numbers at the top and bottom of each rectangle indicate the first and last residues of the transmembrane domain, respectively. The entire sequence of the unique labeled Asp124−Met181 peptide in the CN-1 band, or that of the unlabeled Val349−Met374 or Ile394−Met410 ones from the CN-2 band, are indicated. The position of Arg141 is highlighted. Arrows indicate the sites of proteinase K (Pk) or trypsin (Ti) digestion.

membrane support at the end of the analysis must be associated with an additional, probably N-blocked peptide (or more) that remains to be identified.

Confirmation that MelB residues other than Arg141 are also photolabeled has been obtained by proteolytic mapping of the PAPG-labeled domains of MelB. Gwizdek et al. (*9*) reported that trypsin, or proteinase K, digests MelB at the level of the cytoplasmic loop connecting helices IV−V or that bridging helices VI−VII, respectively, generating complementary fragments that do or do not harbor Arg141 (see Figure 7). Although the results are not illustrated, two salient findings are worth noting. First, both the N-terminal fragment (about 24 kDa) and its C-terminal complement (about 30 kDa) produced by proteinase K digestion carry radioactivity, although only the N-terminal fragment contains Arg141. Second, trypsin digestion also produces two labeled fragments, a moderately labeled 17 kDa N-terminal fragment devoid of Arg141 and a higher radioactive one of 33 kDa (C-terminal) with Arg141. Importantly, labeling of all digested fragments is strongly reduced if excess α-NPG is added during the photolabeling assay.

DISCUSSION

The experiments described in the present study show that the melibiose permease of *Escherichia coli* can be efficiently and selectively labeled with the photosensitive, high-affinity galactosyl analogue [^{3}H]-α-PAPG. Analyses of the rate and/or pattern of radioactivity incorporation in the full-length recombinant MelB-6His permease, in peptides derived by CNBr cleavage or in proteolytic products, indicate that the transporter is labeled at more than one site. One of these domains has been unambiguously identified as the cytoplasmic loop connecting helices IV and V where the label was selectively attached to Arg141.

Two lines of evidence establish that the nitrene-based photoactivatable analogue α-PAPG fulfils the criteria of a specific active-site-directed photoaffinity probe for the melibiose permease. First, [^{3}H]-α-PAPG behaves as a high-affinity substrate for MelB. It is accumulated in RSO membrane vesicles by an energy-driven and uncoupler-sensitive transport mechanism. Its binding to MelB is Na-dependent, with an affinity reaching the micromolar level at saturating concentrations of NaCl. More importantly, [^{3}H]-α-PAPG binding is competitively inhibited by the physiological substrate melibiose or by the high-affinity sugar analogue α-NPG. On the other hand, analysis of the photolabeling characteristics of membrane vesicles containing overexpressed MelB demonstrates that 85% of the label associated with the membrane proteins is covalently attached to a polypeptide (apparent molecular mass 40 kDa apparent) previously identified as the recombinant MelB transporter (*4*). Further characterization of MelB photolabeling was carried out on the recombinant transporter purified by Ni affinity chromatography. An important observation is that melibiose or α-NPG affords nearly complete protection against MelB photolabeling. It is noteworthy that the amount of label associated with the different labeled CNBr-peptides is uniformly decreased on adding melibiose or α-NPG in excess. Thus photolabeling takes place from [^{3}H]-α-PAPG molecules specifically bound to MelB, in accord with the generally accepted definition of active-site-directed photoaffinity.

One of the strategies utilized to identify the MelB domains and/or residues labeled by [^{3}H]-α-PAPG was to purify

labeled His-tagged MelB by affinity chromatography, to submit it to cyanogen bromide cleavage, and then to identify the radioactive CNBr fragments and targeted amino acids therein. Autoradiographic analysis of the CNBr products after electrophoresis shows that the radioactivity was incorporated into two bands, a well-resolved one of 5.5 kDa (CN-1 fragment) and a diffuse one (CN-2) consisting of a mixture of peptides of 2−4 kDa. Sequence analysis of the first 29 amino acids of the CN-1 band unambiguously identified it as the Asp124−Met181 domain in the N-terminal half of MelB. In a topological model of MelB (Figure 7; *7, 8*), this labeled peptide comprises the cytoplasmic loop connecting helices IV−V (loop 4−5), helix V, and almost the full external loop connecting helices V−VI. The presence of such an internal hydrophobic stretch most likely accounts for the faster mobility of the CN-1 fragment relative to that expected from its actual mass (7.5 kDa). On the other hand, the smaller labeled peptides of the CN-2 come from other domains of MelB. These MelB domains are neither the cytoplasmic loop connecting helix X−XI, Val349−Met374, nor the outer loop connecting helices XI and XII, Ile394−Met410, peptides (Figure 7), as no radioactivity release was detected during their sequencing. Examination of the CNBr peptide map of the 30 kDa fragment generated by proteinase K digestion strongly suggests that the Met310−Ile347 (3.7 kDa) and Met374−Gly393 (1.9 kDa) domain in the C-terminal half of MelB are the labeling targets, the other peptide components being too large and devoid of radioactivity. Interestingly, Met310−Ile347 and Met374−Gly393 include helix X and XI, respectively. Evidence has been obtained that they could line the sugar-binding site (*18*). Work is under way to confirm these predictions. Overall, this analysis strongly suggests that discrete domains of both the N- and C-halves of MelB are labeled by [^{3}H]-α-PAPG. This is in line with previous spectroscopic analysis and mutagenesis evidence suggesting that structural components from both the N- and C-terminal domains of MelB contribute to the sugar binding activity (*18*).

Previous structural and/or functional analyses led to the suggestion that the helix IV−loop 4−5 domains of MelB are at or close to the sugar-binding site. Thus Gwizdek et al. (*9*) observed that trypsin cleaves loop 4−5 at the level of the highly charged sequence Asp137−Glu142 carrying the labeled target Arg141. This sequence is thus exposed at the surface of MelB. More interestingly, the two MelB substrates promote cooperative and extensive protection against trypsin cleavage, a finding consistent with a structural rearrangement of the loop domain consecutive to substrate binding. In addition, several point mutations in helix IV and/or loop 4−5 produce marked changes in either the sugar selectivity and/or affinity (Tyr113) or the ionic properties of MelB (Asp124, Gly121) (*14*−*16*, *32*; E. Cordat, G. Leblanc, and I. Mus-Veteau, unpublished results). These findings suggest that some of residues of the helix IV−loop 4−5 domain are either directly involved in sodium and/or sugar binding or indirectly contribute to the coupling interactions between the two binding sites. Preferential incorporation of an active-site-directed photoaffinity probe in loop 4−5 is consistent with both views. However, the actual implication of the selective labeling of Arg141 in loop 4−5 cannot be assessed from the photolabeling data alone. Mutagenesis of Arg141 should be useful in assessing more precisely the Arg141 location relative to the galactosyl-binding pocket as well as its functional role, and also in establishing whether loop 4−5 and/or neighboring helices are directly or indirectly involved in sugar recognition.

It is worth mentioning in this context that Kaback's group recently provided strong evidence that a domain of lactose permease of *E. coli* (LacY) equivalent to helix IV−loop 4−5−helix V in MelB also plays a determining role in sugar recognition by this H^+/sugar transporter (*33*−*39*). MelB and Lac Y have similar 12-transmembrane-domain structures and share several substrates (melibiose, thiomethyl galactoside, α-NPG) (*22*, *38*). In essence, the studies on LacY indicate that Glu126 and Arg144 are irreplaceable for sugar binding. An essential feature is that the two residues are charged-paired residues, suggesting close proximity in the tertiary structure (*34*). A higher resolution topological approach establishes that Glu126 and Arg144 are located at the cytoplasmic end of helix IV or V, respectively, and close to the helix−loop interface (*39*). Replacement of Glu 126 or Arg144 by neutral residues decreases or prevents sugar binding and modifies the reactivity toward *N*-ethylmaleimide of the cysteiyl residue in helix V (Cys148) known to be at the galactosyl binding site. These findings led to the proposal that Arg144, properly oriented as a result of dipolar interactions with Glu126, interacts directly with the sugar. In addition, Glu126 and Arg144 may also play a crucial part in maintaining the conformation of the substrate translocation pathway located in the distal part of LacY (*34*, *40*). Comparison with MelB raises the interesting possibility that specific catalytic determinants of the helix IV−loop 4−5−helix V domain of lacY may have their homologues in the equivalent domain of MelB. In favor of such an idea is the presence an acidic residue (Asp124), essential for MelB function, as Glu126 in helix IV of lacY, also located at the cytoplasmic extremity of helix IV of MelB. Also, arginyl residues (Arg 141 or 149) tentatively located in the loop 4−5−helix V interface of Mel B may well be located on helix V, as for Arg144 in helix V of LacY, and be ion-paired with Asp 124. Extensive mutagenesis of the residue of this MelB domain will allow this attractive hypothesis to be investigated

In conclusion, the ligand-specific photolabeling of the helix IV−loop 4−5−helix domain of MelB together with its biochemical and mutagenesis characterization highlight the importance of this domain for MelB function. Comparison with the structure−function relationships of MelB with that of LacY suggests that, despite a very limited sequence homology, these two sugar transporters with similar secondary structure and substrate specificity, may have conserved domains involved in sugar recognition.

ACKNOWLEDGMENT

We are grateful to Morgane Le Bastard and Raymonde Lemonnier for skillful technical assistance. We also thank Bernard Lagoutte and Pascal Kessler for helpful and valuable discussion during the work.

REFERENCES

1. Pourcher, T., Bassilana, M., Sarkar, H. K., Kaback, H. R., and Leblanc, G. (1990) *Philos. Trans. R. Soc. London B 326*, 411−423.

2. Poolman, B., Knol, J., Van der Does, C., Henderson, P. J., Liang, W. J., Leblanc, G., Pourcher, T., and Mus-Veteau, I. (1996) *Mol. Microbiol. 19*, 911−922.
3. Yazyu, H., Shiota-Niiya, S., Shimamoto, T., Kanazawa, H., Futai, M., and Tsuchiya, T. (1984) *J. Biol. Chem. 259*, 4320−4326.
4. Pourcher, T., Leclercq, S., Brandolin, G., and Leblanc, G. (1995) *Biochemistry 34*, 4412−4420.
5. Reizer, J., Reizer, A., and Milton, H. S. (1994) *Biochim. Biophys. Acta 1197*, 133−166.
6. Poolman, B., and Konings, W. N. (1993) *Biochim. Biophys. Acta 1183*, 5−39.
7. Pourcher, T., Bibi, E., Kaback, H. R., and Leblanc, G. (1996) *Biochemistry 35*, 4161−4168.
8. Botfield, M. C., Naguchi, K., Tsuchiya, T., and Wilson, T. H. (1992) *J. Biol. Chem. 267*, 1818−1822.
9. Gwizdek, C., Leblanc, G., and Bassilana, M. (1997) *Biochemistry 36*, 8522−8529.
10. Mus-Veteau, I., Pourcher, T., and Leblanc, G. (1995) *Biochemistry 34*, 6775−6783.
11. Maehrel, C., Cordat, E., Mus-Veteau, I., and Leblanc, G. (1998) *J. Biol. Chem. 273*, 33192−33197.
12. Lacapere, J. J., Stokes, D. L., Mosser, G., Rank, J. L., Leblanc, G., and Rigaud, J. L. (1997) *Ann. N.Y. Acad. Sci. 834*, 9−18.
13. Tsuchiya, T., and Wilson, T. H. (1978) *Membr. Biochem. 2*, 63−79.
14. Pourcher, T., Zani, M. L., and Leblanc, G. (1993) *J. Biol. Chem. 268*, 3209−3215.
15. Wilson, D. M., and Wilson, T. H. (1992) *J. Bacteriol. 174*, 3083−3086.
16. Zani, M. L., Pourcher, T., and Leblanc, G. (1993) *J. Biol. Chem. 268*, 3216−3221.
17. Hama, H., and Wilson, T. H. (1993) *J. Biol. Chem. 268*, 10060−10065.
18. Mus-Veteau, I., and Leblanc, G. (1996) *Biochemistry 35*, 12053−12060.
19. Cordat, E., Mus-Veteau, I., and Leblanc, G. (1998) *J. Biol. Chem. 273*, 33198−33202.
20. Botfield, M. C., and Wilson, T. H. (1988) *J. Biol. Chem. 263*, 12909−12915.
21. Kotzyba-Hibert, F., Kapfer, I., and Goeldner, M. (1995) *Angew. Chem., Int. Ed. Engl. 34*, 1296−1312.
22. Damiano-Forano, E., Bassilana, M., and Leblanc, G. (1986) *J. Biol. Chem. 261*, 6893−6899.
23. Rudnick, G., Kaback, H. R., and Weil, R. (1975) *J. Biol. Chem. 250*, 1371−1375.
24. Kaczorowski, G. J., Leblanc, G., and Kaback, H. R. (1980) *Proc. Natl. Acad. Sci. U.S.A. 77*, 6319−6323.
25. Fleming, S. A. (1995) *Tetrahedron 51*, 12479−12520.
26. Brandolin, G., Doussière, J., Gulik, A., Gulik-Krzywicki, T., Lauquin, G. J., and Vignais, P. V. (1980) *Biochim. Biophys. Acta 592*, 592−614.
27. Kaback, H. R. (1971) *Methods Enzymol. 22*, 99−120.
28. Ramos, S., Schuldiner, S., and Kaback, H. R. (1979) *Methods Enzymol. 55*, 680−688.
29. Laemmli, U. K. (1970) *Nature 227*, 680−685.
30. Schägger, H., and von Jagow, G. (1987) *Anal. Biochem. 166*, 368−379.
31. Lowry, O. H., Rosebrough, N. J., Farr, A. L., and Randall, R. J. (1951) *J. Biol. Chem. 193*, 265−275.
32. Zani, M. L., Pourcher, T., and Leblanc, G. (1994) *J. Biol. Chem. 269*, 24883−24889.
33. Frillingos, S., Gonzalez, A., and Kaback, H. R. (1997) *Biochemistry 36*, 14284−14290.
34. Venkatesan, P., and Kaback, H. R. (1998) *Proc. Natl. Acad. Sci. U.S.A. 95*, 9802−9807.
35. Sahin-Toth, M., Le Coutre, J., Kharabi, D., Le Maire, G., Lee, J. C., and Kaback, H. R. (1999) *Biochemistry 38*, 813−819.
36. Wilson, T. H., and Wilson, D. M. (1998) *Biochim. Biophys. Acta 1374*, 77−82.
37. Eadie, G. S. (1942) *J. Biol. Chem. 146*, 85−93.
38. Rudnick, G., Schuldiner, S., and Kaback, H. R. (1976) *Biochemistry 15*, 5126−5131.
39. Wolin, C. D., and Kaback, H. R. (1999) *Biochemistry 38*, 8590−8597.
40. Kaback, H. R. (1997) *Proc. Natl. Acad. Sci. U.S.A. 94*, 5539−5543.

BI9916224